Elastic-Plastic Analysis of Suspension Bridge Towers Subjected to Earthquake Ground Motions

By

Yoshikazu YAMADA

(Received April 28, 1961)

This paper deals theoretically with the elastic-plastic analysis of suspension bridge towers subjected to ground motions. In a previous theoretical study it was concluded that the response of the towers of a long span suspension bridge was more significant than that of suspended structures. For convenience of analysis a simplified structural system for a suspension bridge tower with finite degrees of freedom of motion was adopted, and ground disturbances of a simple shape and of an actual earthquake were used. The numerical computation were done on the Kyoto University High Speed Digital Computor, KDC-I. In this investigation some remarkable conclusions on the elastic-plastic response of the system were obtained.

1. Introduction

The method of analysis given in the previous report[1] makes it possible to analyse the earthquake response of a suspension bridge, and provides a complete method for analysis of the dynamic response due to ground motions.

Some fundamental numerical analyses done in previous studies has shown that (1) the motions of a tower subjected to an earthquake are more significant than those of the other parts of a suspension bridge, (2) the natural frequencies of the vibration modes with predominant displacements of the towers are between the vibration frequencies of earthquake motions, and an earthquake disturbance may possibly be resonant with the natural vibrations of the suspension bridge.

Severe earthquakes, therefore, may produce a large amount of deformations which exceed the elastic limit of the material. If the stresses produced by a severe earthquake are to be held within the elastic limit, it would require a considerable amount of construction material in the suspension bridge towers, and such a method of design is not feasible in this case because a destructive earthquake may occur only once in a century or less.

* Department of Civil Engineering

It has been recognized through inelastic analyses of the earthquake resistance of buildings during the past decade, that inelastic deformations absorb a large amount of the vibration energy of the structures. Thus, it is clear that the inelastic deformations of structures are a dominant factor in limiting the forces that develope in a structure due to a severe earthquake.

In the design of a suspension bridge, however, the basic nature of the structure is different from that of ordinary buildings, and the collapse of one tower would cause the catastrophic destruction of the bridge. Plastic deformations, residual deformations, must, therefore, be restricted to magnitudes which will guarantee the safety of the bridge following a destructive earthquake.

In this paper, an approximate method for the elastic-plastic analysis of a suspension bridge tower will first be discussed employing the same kind of physical system used in the previous report. As the process of numerical integration for such systems is quite time consuming, a computer program solution on KDC-I, Kyoto University High Speed Digital Computer, was developed, and numerical computations were done with the computer. The results and their discussion are also given in this paper.

2. Simplification of the Properties of a System

In the inelastic analysis of structures, the first consideration is the material properties such as yield stress and ultimate strength especially for rapidly applied loads. Some experimental results for these are available, but they should not be considered precise. In the following analysis, therefore, the value for the yield stress is taken as the dynamic yield stress, and an idealized stress-strain relation is assumed.

When the idealized stress-starin relation of a perfect elastic-plastic material is assumed for a bending member, the bending moment-curvature relationship shown in Fig. 1 is given theoretically. Curvature is defined as the angle change per unit length. The member bends elastically until the fiber stress of the section reachs its yield value. The curvature increases rapidly as the moment approaches the ultimate capacity M_p'. For analytical design purposes, it is recommended that a reduced capacity be used because considerable curve is required for the section to reach its ultimate capacity[2].

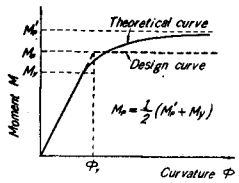

Fig. 1. Moment-Curvature Relationship.

The ultimate moment capacity, in this analysis, will be assumed to be

$$M_p = \frac{1}{2}(M_y + M_p') \qquad (1)$$

$$M_y = \sigma_{dy} S$$

$$M_p' = \sigma_{dy} S_p$$

where, σ_{dy}=dynamic yield stress selected as equal to static yield stress, S=section modulus, S_p=plastic modulus of the section. The momet-curvature relation shown by the dotted line in Fig. 1 will be used in the analysis.

For such a simplified curve, similar to the design curve for limit analysis of structures, plastic hinges form at discrete points at which all plastic rotation occurs. In actuality the plastic domain expands over a length of the member, but the effects of such complicated phenomena are considered beyond the problem under discussion.

The local instability of the tower due to over-loading is also quite important but disregarded in this analysis.

The tower of the suspension bridge is subjected to large axial forces. Ultimate bending capacity of the tower will be affected considerably by the axial force due to dead load and incremental vibration. The interaction curve between the moment capacity M and axial load P is shown in Fig. 2, in which P_p indicates the yielding capacity due to axial force only.

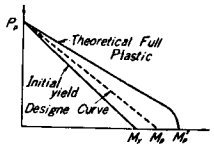

Fig. 2. Interaction Curve for the Tower.

In order to avoid complexity in the analysis, the relation shown by the dotted line in Fig. 2 will be adopted in the analysis. The analytical method for introducing such a relation into the analysis will be given later.

3. Physical System Considered

The system considered is almost the same as that of the previous analysis[1]. If the system in the previous study is used in inelastic analysis just as is, a large number of second order non-linear differential equations have to be solved simultaneously, e.g. for the system in the previous analysis 21 equations. If the system is a linear system, as in the previous analysis, the equation can be solved independently by using the modal analysis shown in the previous paper. For a system having inelastic properties, however, the modal analysis is not applicable and a numerical step-by-step method may be the best method of numerical analysis.

Although general mathematical principles have not been given yet, increasing a number of equations decreases the convergency and stability of the numerical integration, and a smaller time interval for each integration step is required. Therefore the number of equations, the same as the number of discrete points, have to be determined under the following considerations; (1) Characteristics of the problem, (2) Importance of the analytical results, (3) Required accuracy of the results, and (4) Capacity and computing speed of the computer.

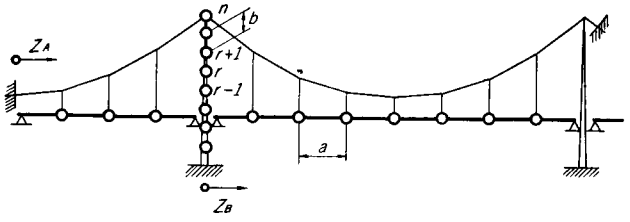

Fig. 3. Physical System Considered.

Giving consideration to these factors, a single tower including some parts of the suspended structures as shown in Fig. 3 was the system adopted in the derivation of the equations. With the derivation of the analysis, motion of the suspended structures is neglected.

4. Equations of Motion

Since the motion of a tower due to earthquake disturbance is of more importance than that of a suspended structure, the equation of motion for the tower of the system shown in Fig. 3 will be discussed.

Adopting the same assumptions for the system as in the previous study, the equations of motion are given as follows. At an inner point of the tower,

$$\frac{W_r}{g}\ddot{y}_r = \frac{1}{b}\left[(M_{r-1}-2M_r+M_{r+1})-(P_{gr}+P_p)(y_{r-1}-2y_r+y_{r+1})\right] \qquad (2)$$

At the top of the tower,

$$\frac{W_n}{g}\ddot{y}_n = \frac{1}{b}\left[M_{n-1}-(P_{gr}+P_p)(-y_n+y_{n-1})\right]+\Delta H \qquad (3)$$

where, W_r=dead load concentrated at the point r, g=gravitational acceleration, y_r=displacement of the point r, b=length of a segment of the tower, M_r=bending moment at the section of the point r, P_{gr}=axial force due to dead load acting at the section r, P_p=increment added to the axial force dne to inertial force, ΔH=horizontal force acting at the top of the tower during vibration.

In Eqs. (2) and (3), ΔH and P_p are due to cable tension and can be determined from the cable equations,

$$\left.\begin{aligned} u_1 &= \frac{H_{p1}L_{E1}}{E_cA_c}-\frac{W_s}{g}\sum y_s \\ u_c &= \frac{H_{pc}L_{Ec}}{E_cA_c}-\frac{W_s}{g}\sum y_s \end{aligned}\right\} \qquad (4)$$

where, u_1=horizontal component of total elongation of the cable of the side span, u_c=horizontal component of total elongation of the cable of the center span, H_{p1}=increment to the horizonal component of side span cable tension, H_{pc}=

increment to the horizonal component of the center span cable tension, L_{E1}=length defined by $\sum(a/\cos^3\alpha_{s,s+1})$ (side span), L_{Ec}=length defined by $\sum(a/\cos^3\alpha_{s,s+1})$ (center span), H_g=horizonal component of dead load cable tension, W_s=dead load concentrated at a point in the suspended structures. Notations of the other quantities such as a, $\alpha_{s,s+1}$, etc. are given in the previous paper[1].

The period of the fundamental natural vibration for a long span suspension bridge in which the vibration of the suspended structures is predominant, is about 10 sec as shown in the previous paper, and the suspended structures are considered to be very flexible. The vibration amplitudes of such structures subjected to earthquakes are not large or rather stand still like the mass of a displacement vibrograph.

Accordingly one assumes, in Eq. (4),

$$y_s = 0 \tag{5}$$

Then,

$$\left.\begin{aligned} u_1 &= (H_{p1}L_{E1})/(E_cA_c) \\ u_c &= (H_{pc}L_{Ec})/(E_cA_c) \end{aligned}\right\} \tag{6}$$

The horizontal components of cable tension are,

$$\left.\begin{aligned} H_{p1} &= (E_cA_cu_1)/L_{E1} \\ H_{pc} &= (E_cA_cu_c)/L_{Ec} \end{aligned}\right\} \tag{7}$$

And the horizontal force acting at the top of the tower is

$$\Delta H = H_{pc}-H_{p1} = E_cA_c[(u_c/L_{Ec})-(u_1/L_{E1})] \tag{8}$$

If the cables on both sides of the tower are fixed at their ends,

$$u_c = -y_n, \qquad u_1 = y_n$$

Then,

$$\Delta H = -E_cA_c[(1/L_{Ec})+(1/L_{E1})]\cdot y_n \tag{9}$$

The incremental axial force acting at the top of the tower is

$$\begin{aligned} P_p &= (H_{pc}+H_{p1})\tan\alpha \\ &= E_cA_c[(1/L_{E1})-(1/L_{Ec})]\cdot y_n\cdot\tan\alpha \end{aligned} \tag{10}$$

If the ground motion on the left side anchorage Z_A is taken into consideration, Eqs. (9) and (10) are modified as follows.

$$\Delta H = -E_cA_c[(1/L_{E1})(y_n-Z_A)+(1/L_{Ec})y_n] \tag{11}$$

$$P_p = E_cA_c[(1/E_{E1})(y_n-Z_A)-(1/L_{Ec})y_n]\tan\alpha \tag{12}$$

Moments in Eqs. (2) and (3) can be obtained by the following equation.

$$M_r = -\frac{B_r}{b}(y_{r-1}-2y_r+y_{r+1}) \tag{13}$$

where, B_r=bending stiffness at the section r in the tower. Inelastic properties of the moments are also taken into consideration and will be discussed in the following section.

5. Considerations on Inelastic and Non-linear Properties

Using Eq. (10) or (12) in Eq. (2), the non-linearity due to the incremental axial forces is taken into consideration.

To avoid complexity of numerical computation, the cable tensions are assumed to be always within the elastic limit. Whenever the computation is carried out, it must be verified whether this condition is satisfied or not.

The elastic-plastic property of the bending moment of the tower is considered to be concentrated at each hinged point considered. Since the plastic hinges occur at discrete points, assuming an elastic-plastic relation, this assumption restricts these discrete points to the hinged points considered. Dividing the tower into a sufficiently large number of segments, a highly accurate analogy to the tower can be made, and the positions at which the plastic hinges yield can be precisely determined. If the number of the divided segments is not large enough, the accuracy of the analysis might be more or less unsatisfactory.

The moment considered does not always retrace its values when the system displaces with velocities of opposite signs. Fig. 4 shows this relation, hysteretic relation, between angle change and the moment M_r. The moment in Eqs. (2) and (3) have this elastic-plastic hysteretic relation, and this relation can easily be considered in the computer program.

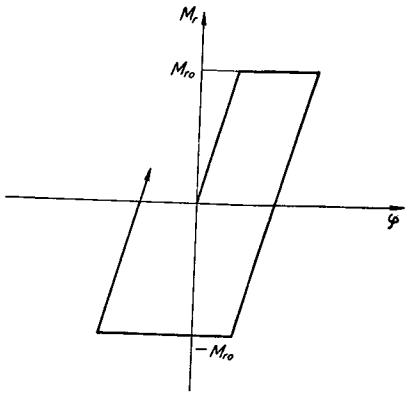

Fig. 4. Moment-Curvature Relation.

Considering this relation, the restoring moment M_r must be less than M_{r0}, the yield moment. Using the following considerations in the computation, the inelatic hysteretic relations on the restoring moment M_r are taken into the analysis.

$$\left.\begin{array}{lllll} & \text{If} & (M_{r,i-1}+\Delta M_{r,i}) \geqq M_{r0} & \text{then} & M_{r,i} = M_{r0} \\ \text{or} & \text{if} & (M_{r,i-1}+\Delta M_{r,i}) \leqq -M_{r0} & \text{then} & M_{r,i} = -M_{r0} \\ \text{or} & \text{if} & |M_{r,i-1}+\Delta M_{r,i}| < M_{r0} & \text{then} & M_{r,i} = M_{r,i-1}+\Delta M_{r,i} \end{array}\right\} \tag{14}$$

The relation between the axial force and the yield moment M_{r0} is given by the following equation under the assumption already made and shown in Fig. 2.

$$M_{r0} = M'_{r0}\left(1-\frac{P_{gr}+P_p}{P_{Yr}}\right) \tag{15}$$

where, M'_{r0}=yield moment of the section r under no axial load, P_{Yr}=the axial force which produces yield stress.

6. Method of Numerical Integration

The analysis was performed on the Kyoto University Digital Computer, KDC-I, using a numerical method of integration described by Prof. Newmark[3].

For the second order differential equation of motion the procedure of integration is shown in the following equations.

$$y_{r,i+1} = y_{r,i}+\dot{y}_{r,i}h+\left(\frac{1}{2}-\beta\right)\ddot{y}_{r,i}h^2+\beta\ddot{y}_{r,i+1}h^2 \tag{16}$$

$$\dot{y}_{r,i+1} = \dot{y}_{r,i}+\frac{1}{2}(\ddot{y}_{r,i}+\ddot{y}_{r,i+1})h \tag{17}$$

Steps of calculation are as follows.

(1) Assume values of the acceleration for each mass at the time $t=(i+1)h$, i.e. assume $\ddot{y}_{r,i+1}$.

(2) Compute the velocity and the displacement of each mass at the time $t=(i+1)h$ from Eqs. (16) and (17).

(3) For the computed velocities and displacements compute the accelerations from the fundamental equations of motion, Eqs. (2) and (3).

(4) Compare the derived acceleration with the assumed acceleration. If these are different, repeat the calculation with the derived acceleration.

7. Description of Program for the Solution on KDC-I

The method described has been programmed for solution on KDC-I.

The method of numerical integration developed by Newmark is applicable to any kind of system of second order differential equations. The program of "Solution of n-Simultaneous Second Order Differential Equations by Newmark's Method (NEWM)" was programmed by the author for $\beta=1/6$ and listed as one of the KDC-I Subroutines[4].

The subroutine (NEWM) includes the steps (1), (2), and (4) given in previous article and requires two auxiliary routines. One is the routine of computation of the accelerations from the fundamental equations of motion, step (3), and the other is the routine of printing the computed results in the given format.

Two different programs have been prepared for the routine of printing the

computed results. The first provides results for the complete history of the dynamic response of the system, while the other can be used to determine only the maximum and minimum responses during the time history of the system.

The computer program for the computation of either the complete history of the response or the maximum and minimum dynamic responses consists of four parts of instructions and two parts of data. These are,

(MAIN) : Main controlling routine.

(NEWM) : Subroutine of the solution of simultaneous second order differential equations.

(AUX) : Computation of accelerations from the fundamental equations of motion.

(PRINT) : Type A—Printing the results at the end of each step and storing the external ground disturbances necessary at the advanced step of computation.

Type B—Selecting the maximum and minimum responses at the end of each step and storing the external ground disturbance necessary at the advanced step. When the computation is finished, print out the maximum and minimum responses.

(DATAI) : Data showing structual properties.

(DATAII) : Data of ground motion.

In Fig. 5 is shown a general flow diagram of the computation. The detailed flow diagrams and the write up of the complete program are omitted in this paper.

In the case of the maximum and minimum dynamic response computation, the following dynamic responses were given.

(1) The maximum dynamic response of the absolute value of displacements.

(2) The maximum and the minimum dynamic responses of momets.

(3) The maximum and the minimum dynamic responses of curvatures multiplied by b, i.e. the maximum and the minimum $(-y_{r-1}+2y_r-y_{r+1})$.

If no plastic deformations are yielded, the maximum and the minimum moments are proportional to the maximum and the minimum responses of curvatures.

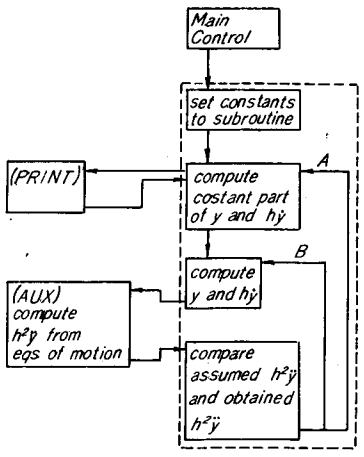

Route A : step to the next time interval
Route B : iteration

Fig. 5. Main Diagram.

Required computing time for one step of computation during $t=nh$ and $t=(n+1)h$ is found by using the program of time history, Program Type A, to be about

$$1000\,s+21000\ (ms)$$

in which $1000s$ is the computation time and 21000 is the printing time, and s indicates the number of iterations. The value of s varies depending upon the error criterion δ, and it is preferably selected so as to be 5 or 6. Substituting $s=5$ into the above exprssion, the average computation time of each time interval is about 5 sec. and the printing time is about 21 sec.

By using the program for the maximum and the minimum responses, Program Type B, the average total computing time required in each step decreased to about 10 sec.

If 400 steps are computed, the total time required is for Type A program 2.9 hours, and for Type B program 1.1 hours.

8. Numerical Example and its Physical Constants

To facilitate numerical computations the Akashi Straits Bridge used in the previous study was selected[5]. A seismic design of the towers of this bridge was done primarily by the classical seismic coefficient method using the seismic coefficient $k=0.2$.

The main dimensions and physical constants of the towers are shown in Fig. 6 and Table 1. The following simplifications of the structure necessary to carry the computer analysis were assumed.

(1) The tower was divided into four segments as shown in Fig. 7.

(2) Physical constants of this simplified system were assumed as shown in Table 2.

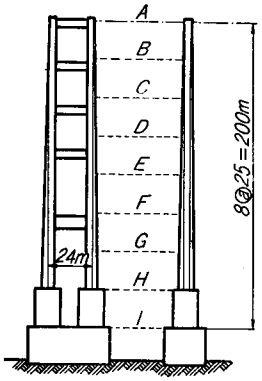

Fig. 6.

Table 1. Dimensions of Tower Sections

Section	width (m)	height (m)	area (m^2)	I (m^4)	weight (ton)
A	3.00	5.00	1.62	3.75	177
B	3.50	5.75	2.25	6.65	455
C	4.00	6.50	2.70	10.99	585
D	4.50	7.25	3.15	17.15	731
E	5.00	8.00	3.60	25.60	893
F	5.50	8.75	4.07	36.85	1071
G	6.00	9.50	4.50	51.44	1266
H	6.50	10.30	4.95	70.00	1476
I	7.00	11.00	5.40	93.17	

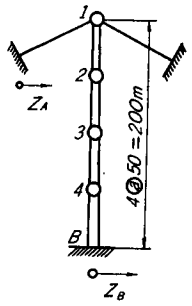

Fig. 7.

Table 2. Properties of Approximate System

Section	W_r (ton)	B_r/b (ton)	M'_{r0} (t-m)	P_{gr} (ton)	P_{Yr} (ton)
1	340			11375	
2	1165	92316	85135	11715	64800
3	1778	215040	161538	12880	86400
4	2521	432096	273022	14658	108000
B		782628	427118	17179	129600

9. Ground Motions

The earthquake motions are quite complicated and it is quite difficult to predict future strong earthquakes. Since no strong motion records are available in Japan, the ground motions used in this numerical analysis are (a) a simple harmonic motion, and (b) the 1957 South California Earthquake.

(*a*) *Ground motion with simple harmonic shape.*

The purpose of the numerical analysis for ground motion with a simple shape is to study the fundamental characteristics of the dynamic response.

The ground motion used has the following shape.

$$\left.\begin{aligned} Z &= A\sin\omega t \qquad 0 \leqq t \leqq T \\ &= 0 \qquad\qquad t > T \end{aligned}\right\} \tag{18}$$

where, $\omega=\dfrac{2\pi}{T}$.

Numerical computations were made for ground motions with period $T=0.6$ sec. and $T=1.2$ sec. The displacement amplitudes A were selected as $A=10$, 20, 30, and 40 cm, and the corresponding maximum accelerations are,

In the case of	$T=0.6$ sec	$T=1.2$ sec.
$A=10$ cm	1.119 g	0.280 g
$A=20$ cm	2.238 g	0.560 g
$A=40$ cm	4.476 g	1.119 g

(*b*) 1957 *So. California Earthquake*

In the analysis of the earthquake response of a suspension bridge, the records of a displacement meter are necessary. Since no strong motion records are available in Japan, the strong motion displacement record of the 1957 South California Earthquake obtained by Carder Displacement Meter was used in this analysis as a numerical example[6]. The ground motion record is given in Fig. 8. The maximum displacement is 1.4 cm and the maximum acceleration obtained by the accelerograph is about 0.17 g.

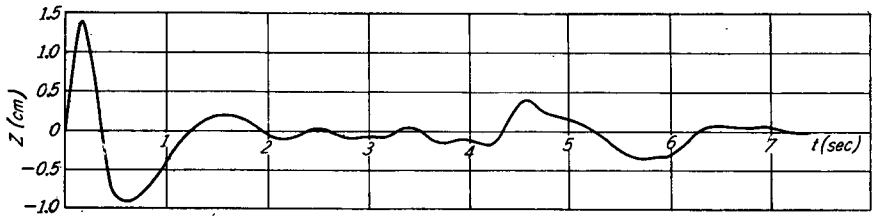

Fig. 8. 1957 So. California Earthquake.

The ground motion of the 1957 So. California Earthquake, however, is not large enough to apply to the elastic-plastic analysis of the suspension bridge tower, so the ground motions magnified by load factors were used in the numerical analysis. These factors were $\alpha=1$, 5, 10, 15, 20, 30, and 40.

10. Numerical Computation and Results Obtained

The time intervals h were selected, considering the accuracies of the process, as follows. For the ground motion of

Sine curve with the period $T=0.6$ sec,	$h=0.01$ sec
Sine curve with the period $T=1.2$ sec,	$h=0.02$ sec
1957 So. California Earthquake	$h=0.018939$ sec

The value of δ which specifies the accuracy of the integative process is selected, in all cases, as $\delta=0.25\times10^{-8}$. Taking this value, the iteration of each step is repeated about five times and δ is considered to be adequate.

(*a*) *History Curves.*

A history curve is a plot of the variation of displacement or moment as a function of time. The curves in Figs. 9 (a) (b) and 10 (a) (b) are for displacements and moments due to the 1957 So. California Earthquake magnified by load

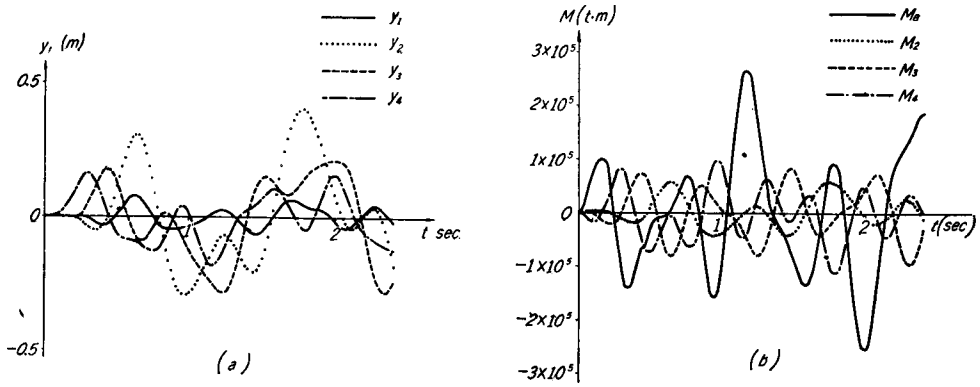

Fig. 9. History Curves. (Load Factor 10)

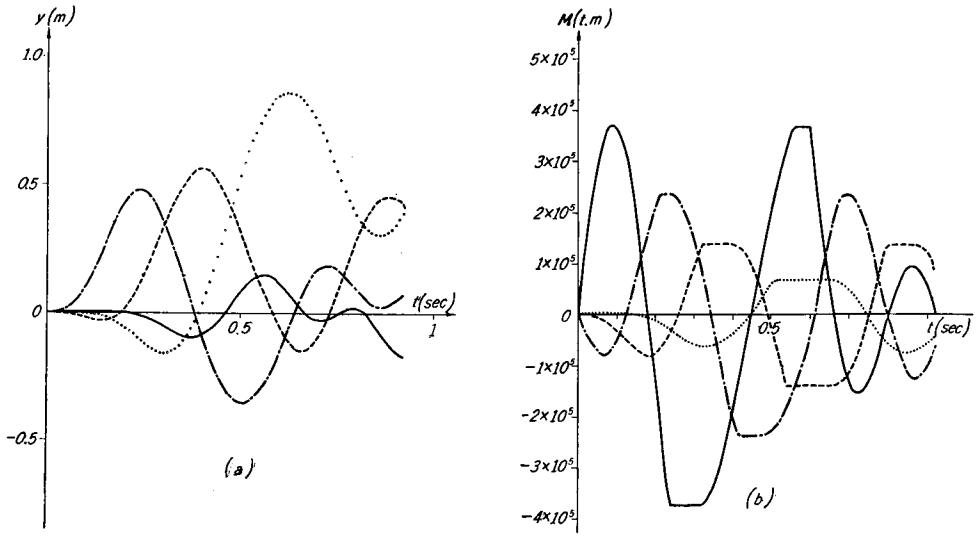

Fig. 10. History Curves. (Load Factor 40)

factors 10 and 40 respectively. In these curves the dynamic response given by the computer are plotted and the specific curves shown by the series of small open circles in these history curves, y_2 and M_2 curves, are the direct plotting of the computer outputs. Some history curves due to simple harmonic ground motions were also obtained, but are omitted in this paper.

(*b*) *Maximum Dynamic Response*

Maximum dynamic response obtained on KDC-I are summarized in Tables 3 through 5. In these tables the maximum moment and the maximum curvature are the maximum dynamic resposes of their absolute values.

These maximum values are the maximum dynamic responses during the first few seconds of the dynamic history specified by the total number of steps in the time intervals. For simple harmonic ground motion with period $T=0.6$ sec. $T=1.2$ sec. and for the 1957 So. California Earthquake, these numbers of steps were chosen as 130 steps (1.3 sec), 130 steps (2.6 sec), and 380 steps (7.2 sec) respectively.

Fig. 11 shows the relations of the maximum displacements and the load factors, and Fig. 12 shows the relations of the maximum moments or maximum curvatures and the load factors for the 1957 So. Calif. Earthquake.

(*c*) *Moment-Curvature Relation*

As already mentioned, the maximum and minimum bendibg moments and the corresponding curvatures were obtained on KDC-I. Although complete time history curves are necessary to obtain the complete moment-curvature relations,

Table 3. Maximum Response due to Ground Motion of Eq. (18), $T=0.6$ sec

A (m)	Response			
	Maximum Displacements (m)			
	y_1	y_2	y_3	y_4
0.1	0.06950	0.29515	0.15818	0.16435
0.2	0.12919	0.48090	0.27989	0.24551
0.4	0.16844	0.86065	0.55976	0.47640
	Maximum Moments (ton-m)			
	M_2	M_3	M_4	M_B
0.1	54678.18	87485.34	75454.37	257245.61
0.2	69960.80*	137750.37*	153668.49	370240.31*
0.4	69690.99*	137790.00*	236288.50*	370942.54*
	Maximum Curvature (Multiplied by b)			
	$\varphi_2 b$	$\varphi_3 b$	$\varphi_4 b$	$\varphi_B b$
0.1	0.59229	0.40683	0.177824	0.32870
0.2	0.66861*	0.51249*	0.35564	0.49102*
0.4	1.81452*	1.20352*	0.68391*	0.72526*

* where the plastic hinge is yielded.

Table 4. Maximum Response due to Ground Motion of Eq. (18), $T=1.2$ sec

A (m)	Response			
	Maximum Displacements (m)			
	y_1	y_2	y_3	y_4
0.1	0.038829	0.312723	0.250845	0.108106
0.2	0.077416	0.625976	0.484436	0.216213
0.3	0.116371	0.773533	0.644242	0.324319
0.4	0.136554	0.844889	0.606817	0.432424
	Maximum Moments (ton-m)			
	M_2	M_3	M_4	M_B
0.1	36949.98	45210.25	67619.10	167156.60
0.2	69560.96*	89249.75	135213.92	334295.54
0.3	69943.25*	109958.54	185490.05	369887.11*
0.4	69975.85*	127908.24	204575.99	369636.36*
	Maximum Curvatures (Multiplied by b)			
	$\varphi_2 b$	$\varphi_3 b$	$\varphi_4 b$	$\varphi_B b$
0.1	0.400255	0.210241	0.156491	0.213584
0.2	0.802689*	0.415038	0.312926	0.427145
0.3	1.009824*	0.511340	0.429280	0.473491*
0.4	1.393774*	0.594811	0.473450	0.483583*

Table 5. Maximum Earthquake Response
Standard Earthquake: 1957 So. California Earthquake

Load Factor	Response			
	Maximum Displacements (m)			
	y_1	y_2	y_3	y_4
1	0.008696	0.043824	0.035070	0.018215
5	0.043515	0.21911	0.17536	0.09107
10	0.087116	0.43819	0.35073	0.18212
15	0.11664	0.64353	0.43419	0.24293
20	0.13238	0.85599	0.49891	0.32391
30	0.17243	1.20856	0.67451	0.48615
40	0.17649	1.48928	0.86365	0.63521
	Maximum Moments (ton-m)			
	M_2	M_3	M_4	M_B
1	6311.45	10812.34	11487.72	27261.96
5	31551.75	54061.56	57438.18	177703.93
10	63089.32	108121.04	114869.73	272641.52
15	69998.95*	137332.84*	164109.12	344732.91
20	70050.22*	137663.69*	178498.82	345871.69
30	70140.29*	137767.24*	236130.87*	370804.85*
40	70143.31*	137838.01*	236175.79*	370996.71*
	Maximum Curvatures (Multiplied by b)			
	$\varphi_2 b$	$\varphi_3 b$	$\varphi_4 b$	$\varphi_B b$
1	0.068368	0.050281	0.026586	0.034834
5	0.34178	0.25140	0.13293	0.22726
10	0.68341	0.50280	0.26594	0.34837
15	1.01864*	0.65397*	0.37980	0.44048
20	1.49461*	0.81745*	0.41310	0.44193
30	1.93737*	1.07380*	0.57448*	0.56058*
40	2.29241*	1.25193*	0.72752*	0.82444*

Table 6. Maximum Earthquake Response
Standard Earthquake: 1957 So. California Earthquake, $Z_A = -Z_B$

Load Factor	Response			
	Maximum Displacements (m)			
	y_1	y_2	y_3	y_4
10	0.17449	0.39172	0.31017	0.17986
20	0.32362	0.72961	0.39808	0.33033
40	0.51560	0.88772	0.76559	0.64628
	Maximum Moments (ton-m)			
	M_2	M_3	M_4	M_B
10	61887.18	111467.92	111612.81	271970.51
20	70219.92*	137898.89	159828.98	347521.17
40	70837.37*	139033.51*	238376.34*	369794.40*
	Maximum Curvatures (Multiplied by b)			
	$\varphi_2 b$	$\varphi_3 b$	$\varphi_4 b$	$\varphi_B b$
10	0.67038	0.51836	0.25831	0.34751
20	1.38915*	0.85358	0.36989	0.44404
40	1.41968*	1.42920*	0.72907*	0.88568*

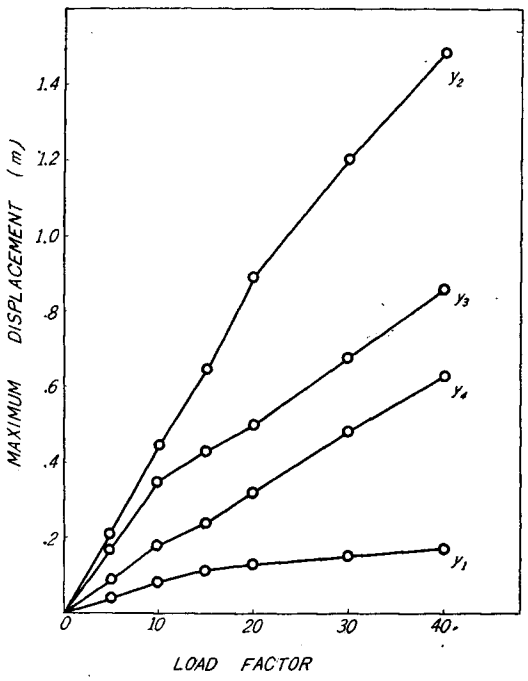

Fig. 11. Maximum Displacements.

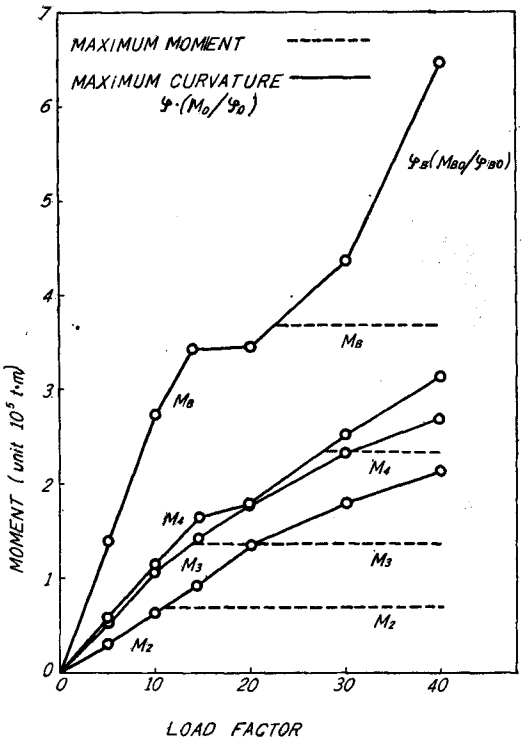

Fig. 12. Maximum Moments and Maximum Curvatures.

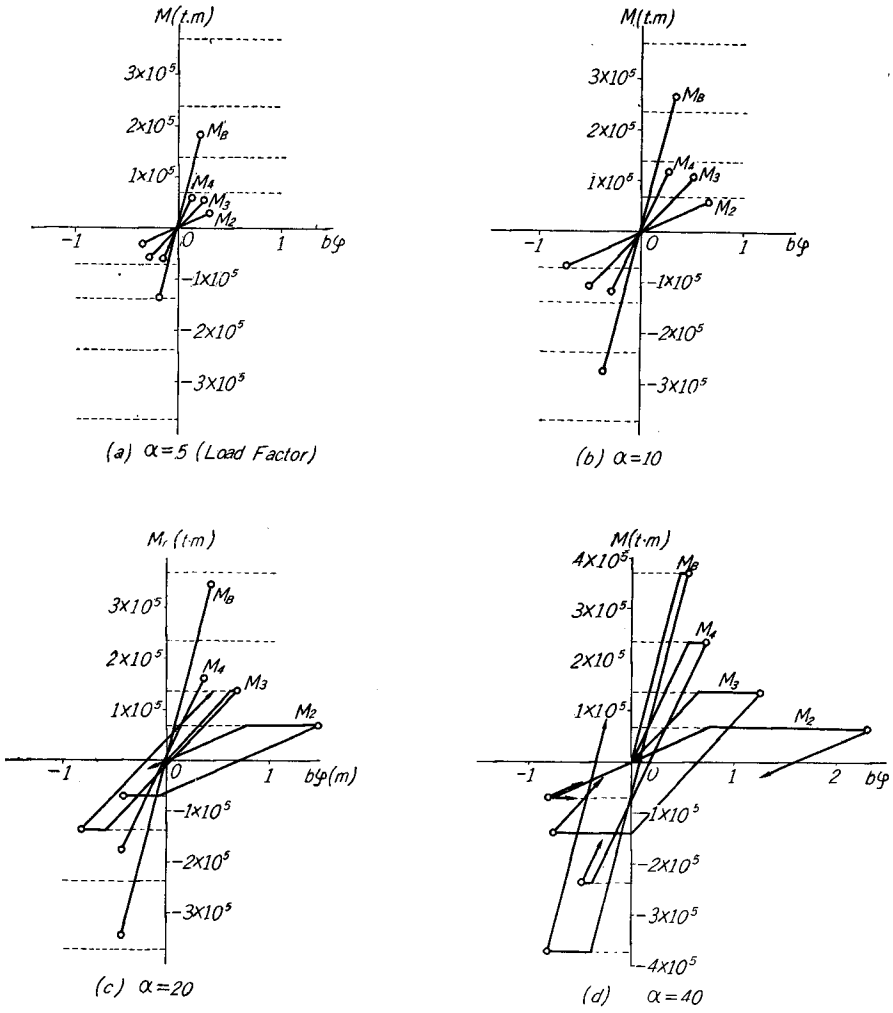

Fig. 13. Hysteresis Curves.

hysteresis relation, the outlines of these relations can be roughly estimated from the maximum and minimum response obtained.

Figs. 13 (a) through (d) are the moment-curvature relations obtained from the maximum and minimum outputs due to the 1957 So. California Earthquake. The open circles in Figs. 13 (a) through (d) were the values of outputs of the computer, and the hysteresis curves were estimated from these points. The yield lines of these figures are not straight lines but functions of axial force, through the influence of axial force is quite small, and these effects were disregarded in these figures,

(*d*) *Effects of Motion of Anchorage*

A program was first provided for the solution of the dynamic response of the tower subjected to the ground motion acting at the tower base. In the numerical computation described thus far, the ground motions were considered to act only at the base of the tower, and the left side anchorage was assumed to stand still.

Effects of the motion of the left side anchorage, Eqs. (11) and (12), can be considered by slight modifications of the computer program. Because of the long span length of the suspension bridge, any phase difference between the disturbances is possible. In the modified program, the ground motions are assumed to have opposite directions, and are given as $Z_A = -Z_B$. Because of the non-linearity of the system, the method of summing up the effects which was used in the linear analysis is not applicable in this analysis.

Using the modified program and assuming the phase relation given, time history curves due to the 1957 So. California Earthquake were obtained as shown in Figs. 14 (a) and (b). The maximum dynamic responses obtained under the same assumptions are tabulated in Table 6.

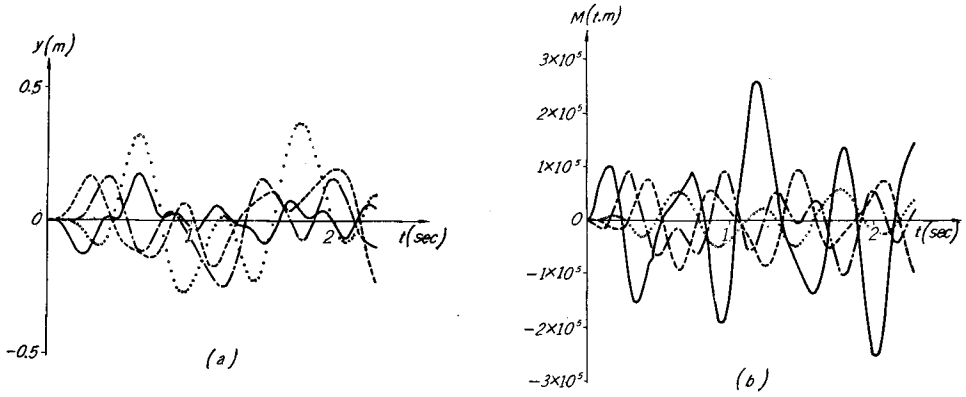

Fig. 14. History Curves. (Load Factor 10)

Comparing Figs. 14 (a) and (b) to Figs. 9 (a) and (b), the dynamic response curves for the two cases are quite similar, except the response of the displacement at the top of the tower. The maximum responses shown in Table 6 appear to be slightly greater or less than the values in Table 5 except for the response at the top of the tower.

11. Conclusion on the Results Obtained

Some of the remarkable conclusions derived directly from the numerical computations will be summarized as follows.

(1) The large energy dissipation due to plastic deformations affect the maximum dynamic responses which do not proportionally increase with the ground motion in the range where plastic deformations occur. Although some considerations of the allowable plastic deformations of the tower are necessary, the effects of plastic deformations are significantly important not only in the design of the tower but in the design of substructures.

(2) Influence of incremental axial force to elastic response given in the form of $P_b(y_{r-1}-2y_r+y_{r+1})$ is not important since the maximum dynamic response within an elastic range is approximately a straight line.

(3) In the analysis given, the yield moments of the cross section were considered to vary with the axial force. Numerical values of yield moments obtained from the dynamic respone of the bending moments indicated a slight variation in those values, and they are approximately considered to be invariable and plotted on straight lines in the figures.

(4) Comparing the maximum responses due to the ground disturbances with different periods but with the same maximum ground acceleration, such as the ground motions with $T=0.6$ sec. $A=10$ cm and with $T=1.2$ sec $A=40$ cm, the maximum ground acceleration is no longer a proper indication of the earthquake intensity for the suspension bridge analysis. It seems possible to conclude from a comparison of the maximum responses due to ground motions with different perions but with the same amplitude that the suspension bridge towers are flexible type structures. This comparison, however, is done only for two cases, $T=0.6$ and 1.2 sec. and further investigations are necessary to obtain a general conclusion on the effects of the periods of external disturbances.

(5) As shown in the preceding article, the effects of the motion of the anchorage are not significant in the analysis of the tower, and it is approximately possible to disregard the effects.

12. Concluding Remarks

An analytical method concerning the elastic-plastic dynamic response of the suspension bridge towers was derived, and some conclusions given in the preceding article were obtained.

Because the system considered has only four degrees of freedom, the results obtained may not have sufficiet accuracy. The results obtained, however, show the fundamental nature of the response. A more accurate analysis of such systems will be the subject of future work.

The earthquake ground motion employed has only a single predominate ground displacement as shown in Fig. 8, and the effects of dynamic resonance

within the system were not emphasized in the response obtained. Some actual earthquakes have a considerable number of cycles of predominate vibration, such as the 1940 El Centro Earthquake. Responses to such earthquakes will also be tracted in future studies.

Acknowledgment

The author would like to express his appreciation to the Kyoto University Computer Center for the use of KDC-I in carrying out the computations in this study. He also would like to express his appreciation to Dr. Chujiro Haraguchi, the Mayor of the City of Kobe, and Professor Ichiro Konishi to whom he is greatly indebted for the completion of this work.

Bibliography

1) Konishi, I. and Yamada, Y.: THIS MEMOIRS **22**, 277 (1960)
2) Norris, C. H. and others; "Structural Design for Dynamic Loads", McGraw-Hill, 8 (1959)
3) Newmark, N. M. ; Proc. of ASCE, **85**, EM, 67 (1959)
4) KDC-I Library, KDC-I Manual III, p. 75, Kyoto University Computer Center (1961)
5) Haraguchi, C.; The Proposed Suspension Bridge Over the Akashi Straits to Connect Kobe City with Awaji Island, Kobe City (1959)
6) United State Earthquakes 1957, U. S. Government Printing Office, 97 (1959)